

# Single Molecule Force Spectroscopy of Azobenzene Polymers: Switching Elasticity of Single Photochromic Macromolecules

Nolan B. Holland,<sup>†,§</sup> Thorsten Hugel,<sup>†</sup> Gregor Neuert,<sup>†</sup> Anna Cattani-Scholz,<sup>‡</sup> Christian Renner,<sup>‡</sup> Dieter Oesterhelt,<sup>‡</sup> Luis Moroder,<sup>‡</sup> Markus Seitz,<sup>†</sup> and Hermann E. Gaub<sup>\*,†</sup>

*Lehrstuhl für Angewandte Physik & Center for Nanoscience, Ludwig-Maximilians-Universität, Amalienstrasse 54, 80799 München, Germany, and Max-Planck-Institut für Biochemie, Am Klopferspitz 18 a, 82152 Martinsried, Germany*

*Received July 17, 2002; Revised Manuscript Received November 22, 2002*

**ABSTRACT:** The reversible, optical switching of individual polymer molecules was observed using molecular force spectroscopy. We synthesized a polypeptide with multiple photoactive azobenzene groups incorporated in the backbone. The contour length of the polymer could be selectively lengthened or shortened by switching between the *trans*- and *cis*-azo configurations with 420 and 365 nm wavelength light, respectively. This *cis*- to *trans*-azo configurational transition induced by ultraviolet light resulted in a measurable change in polymer contour length. The contour length change was observed at low force and under external loads of up to 400 pN using a modified force spectrometer, in which the sample could be irradiated in total internal reflectance. The ability to shorten the polymer against an external load is the first demonstration of photomechanical energy conversion in an individual molecule. This is a significant milestone in the road toward molecular level machines.

## Introduction

Reversible transformations in chemical species induced by photoexcitation have attracted much attention owing to their high potential for application in various optoelectronic devices, e.g., optical memory, photooptical switching, and display.<sup>1–5</sup> One such extensively studied molecular process is the *trans/cis* (or *E/Z*) configurational transition of double bonds, such as found in the stilbene or the azobenzene moiety. This photoinduced isomerization between the extended (*trans*) and the compact (*cis*) configurations is reversibly triggered at two different wavelengths of light and thus could be utilized as a light triggered switch.<sup>2,6</sup> It was the basis for the first artificial example of light-driven ion transport through membranes<sup>7</sup> and has since been frequently used in synthetic photoresponsive systems for regulating the geometry and function of biomolecules<sup>8–10</sup> and organic materials<sup>4,5,11,12</sup> as well as supramolecular complexes.<sup>13–15</sup>

In technological applications, the change in the absorptive properties upon photoisomerization has made azobenzene-based fast response liquid crystals successful for image storage devices,<sup>16</sup> and azobenzene side-chain polymers have proven to be an ideal material for erasable holographic data storage.<sup>17–20</sup> In addition, the reversible geometric change (lengthening and shortening) of the azobenzene chromophore upon photoisomerization may result in significant photomechanical effects, as this has been demonstrated for azobenzene polymers in bulk and solution.<sup>21–27</sup> For example, when azobenzene groups are incorporated into the backbone of a polymer, photoinduced changes in the hydrody-

namic radius of the polymer coil were observed by viscosity measurements. Rigid linkers between the azobenzene moieties resulted in particularly large reversible changes of up to 60%.<sup>23</sup> While photomechanical effects have been utilized in bulk polymer materials, particular interest arises from their potential use for the construction of molecular machines in nanotechnology.

Biological molecular motors are capable of performing specific tasks in response to specific external energy sources in a highly sophisticated fashion<sup>28–32</sup> and thus may soon be utilized in nanoscopic devices. However, the design of synthetic molecular machines is just beginning to be explored.<sup>33–39</sup> Photons have been proposed as an ideal primary energy source because their application is fast, well controlled, and “clean”; i.e., it normally does not result in byproducts if used at moderate levels.<sup>40</sup> The ability to convert optical excitation energy into molecular motion thus makes photochromic molecules such as azobenzene highly promising for the development of synthetic molecular level machines.

The investigation and use of nanoscopic optomechanical energy transducers require interfacing them with the macroscopic world. In the past decade, mechanical experiments with single macromolecules in solution have become possible in a wide dynamic range and with an accessible force window from entropic forces at several femtonewtons (fN) to the rupture of covalent bonds above a nanonewton (nN).<sup>41–51</sup> It has been demonstrated for many systems that, with these tools, small differences in polymer length and minute forces generated by conformational changes can be directly measured; likewise, conformational transitions can be induced along polymer chains by mechanical stress, upon which the molecule's elastic properties may undergo marked changes.<sup>51–54</sup> Such transitions in the polymer chains have been described as a series of elastically coupled two-level systems, each representing

\* To whom correspondence should be addressed: e-mail [gaub@physik.uni-muenchen.de](mailto:gaub@physik.uni-muenchen.de).

<sup>†</sup> Ludwig-Maximilians-Universität.

<sup>‡</sup> Max-Planck-Institut für Biochemie.

<sup>§</sup> Current address: Department of Physiology and Biophysics, Case Western Reserve University, 10900 Euclid Avenue, Cleveland, OH 44106.

one individual segment (or module) of the polymer chain.<sup>55</sup> These developments open the possibility of studying the photoisomerization of azobenzene by atomic force microscopy (AFM)-based force spectroscopy, when many chromophores are incorporated into a polymer backbone to amplify the photomechanical effect in a single chain.

In this paper, we describe the coupling of optical excitation with AFM force spectroscopy, utilizing an object slide as a waveguide. With this combined experimental setup, it is possible to measure the mechanics of single photochromic polymers precisely and simultaneously to their manipulation by optical excitation. We thoroughly characterized a polyazopeptide, observed reversible length changes of single chains as induced by light of different wavelengths, and also studied this process under the influence of an external stretching force. Our findings provide the first experimental basis for controlled optomechanical energy transduction and optical information storage at the level of individual molecules employing synthetic photochromic polymers.

## Experimental Section

**AFM Setup with Optical Excitation.** Single molecule force spectroscopy was performed on a home-built instrument and a modified Molecular Force Puller (Asylum Research, Santa Barbara, CA). In each instrument the tip sample separation is controlled by a one-dimensional piezo equipped with a position detector. Using the measured value of the sample position allows us to eliminate any contribution of piezo drift to our measurements. Microlevers (Thermomicroscopes, Sunnyvale, CA; nominal spring constants: 13 and 30 mN/m) were coated by thermal evaporation with 5 nm of chrome–nickel (80:20) followed by 50 nm of gold to allow for the chemical binding of the thiol ends of the polymers. The spring constant of each cantilever was calibrated prior to use by measuring the amplitude of the thermal oscillations.<sup>56</sup>

We redesigned the sample stage in order to couple optical excitation with measurements of the mechanical response of a single polymer molecule. The general concept of the design is that the sample is attached to a glass microscope slide, which is used as a waveguide (Figure 1). The light of a xenon flashlamp JML-C1 (Rapp OptoElectronic, Hamburg, Germany) with a pulse length of 1 ms was filtered either by a 365 nm band-pass filter (band half-width = 12.2 nm, maximum pulse energy  $E_{\text{max}} = 10$  mJ) for *trans*- to *cis*-azo switching or a GG 420 nm colorglass filter ( $E_{\text{max}} = 100$  mJ) for *cis*- to *trans*-azo switching. In addition, a colorglass BG12 blocked long wavelength excitation. The light was focused onto the polished edge of the microscope slide. The energy of the light pulse before entering the object slide was measured by a Thermal Power Meter (Spectra Physics, model 407A). The evanescent wave from total internal reflection of the excitation light beam passing through the slide irradiates the sample while interactions with the cantilever are minimized. Total internal reflection was of crucial importance to eliminate the deleterious effects of absorption by and thermal heating of the cantilevers. The measurements were performed in dimethyl sulfoxide (DMSO), which has a refractive index of 1.48; therefore, high refractive index flint glass slides (F-2, Schott Glas Mainz, Hellma Optik GmbH Jena,  $n_D \sim 1.666$ ) were necessary to satisfy conditions for total internal reflection as well as to provide high transmission in the UV.

Various test measurements were performed to exclude artifacts which might arise from several sources, including solvent effects and cantilever response to excitation light. The effect of a light pulse on the deflection signal in the absence of any polymer molecule was analyzed. Direct illumination of the sample resulted in such a strong interaction with the cantilever that the resulting cantilever deflection (corresponding to several nanonewtons of force) would result in a rupture of polymer attachment. This is why the total internal reflection

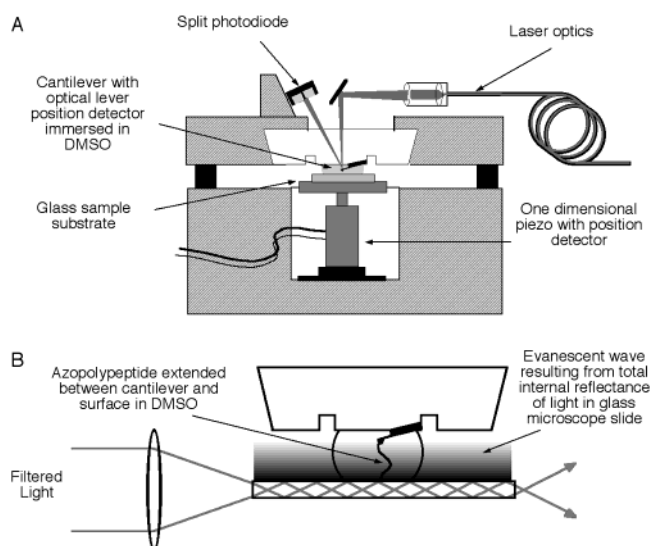


**Figure 1.** Schematic of the optomechanical experimental setup. A flint glass microscope slide is used in a dual role as a sample substrate for the force spectrometer (A) and as a waveguide for generating an evanescent field to excite the polymer sample (B). Light is generated using a flash lamp, and the desired ultraviolet wavelengths are chosen with band-pass filters. An additional high pass filter eliminates low-frequency radiation. The filtered light is directed into a polished end of the microscope slide at a low enough angle to result in total internal reflectance. The polymer sample, which is covalently attached to the cantilever spring tip and the glass slide, is excited by the evanescent wave while its mechanical properties are probed using the force spectrometer.

geometry is necessary. With the given length of the cantilever tip of several microns, the penetration depth of the evanescent field (wavelength  $(\lambda)/2\pi \sim 50$  nm) is short enough to prevent interaction with the cantilever itself. Nonetheless, we observed further artifacts in the deflection signal from the lamp (Figure 2A,B), which were eliminated with careful experimental setup (Figure 2C,D) as described below in detail. No matter how carefully the light was coupled into the sample, stray light during the pulse reaches the photodiode, which detects the cantilever position. This appears as a 1 ms spike in the deflection signal but does not correspond to any cantilever motion or interfere with our measurements. A second artifact was observed as a small deflection which decays back to equilibrium on a time scale of seconds. As this only occurred in certain instances, when the light was not coupled well into the sample slide, it is believed to be caused by light energy being absorbed by the cantilever, resulting in a thermal bimetal effect. The final artifact was a damped oscillation in the deflection-time signal starting a few milliseconds after the light pulse and lasting several hundred milliseconds. This was caused by acoustic and vibrational noise from the flash lamp. By acoustically and mechanically decoupling the lamp from the AFM and shielding all light that is not coupled into the flint glass, we were able to reduce the detrimental artifacts below the thermal noise level (Figure 2C,D).

Further control experiments were performed to identify possible thermal side effects on the force vs extension curves of single polymer chains, which may be a result of the ultraviolet irradiation. While any thermal energy deposited on the molecule directly would be dissipated into the bulk medium at frequencies much faster than the time scale of our experiments, thermal effects resulting from heating of solvent or glass substrate cannot be excluded a priori. To fully exclude such thermal effects (as well as other possible irradiation artifacts affecting the measurement of single chain elasticity), control measurements were performed on polysaccharides, which do not contain photochromic molecular units. No measurable effects were observed in the force–extension curves of these polymers (Figure 3). These data also demon-

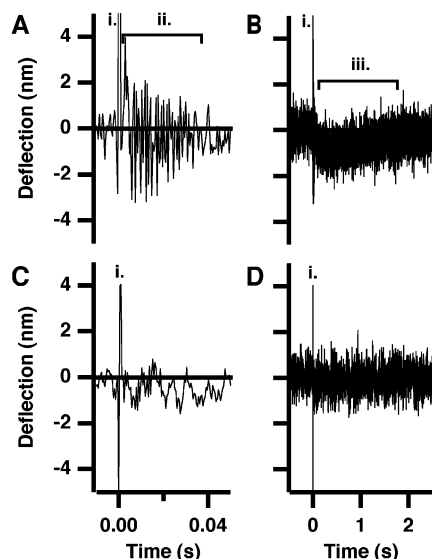


**Figure 2.** Interaction of light pulse with cantilever beam. The deflection signal of the cantilever probe vs time when a single flash of 420 nm wavelength light is coupled into the spectrometer reveals the successful isolation of the cantilever from the excitation. A setup where the coupling of the light into the sample slide is not ideal (A, B) shows significant interactions with the cantilever, including the initial light pulse impinging on the position sensing photodiode at  $t = 0$  (i), the mechanical and acoustic noise arriving several milliseconds after the pulse (ii), and a presumably thermal interaction occurring on the time scale of seconds (iii). When the light pulse is well-coupled (C, D), the only signal observed is light pulse reaching the photodiode (i). The deleterious interactions with the cantilever are eliminated.

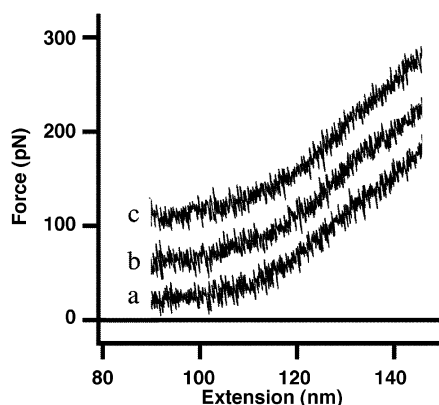
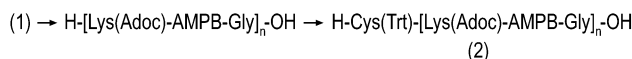
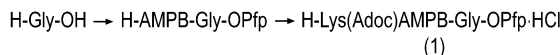
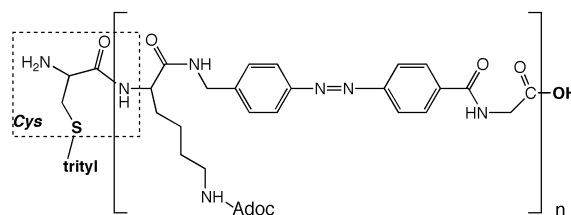


**Figure 3.** Effect of light pulses on polysaccharide molecule force traces. Three traces of the same polysaccharide molecule before excitation (a) and after excitation with light pulses of 365 and 420 nm wavelength (b and c, respectively) show no significant change in the force profile. This clearly demonstrates that the light pulse has no effect for a nonphotoactive molecules. Force trace (b) and (c) have been shifted by 40 and 80 pN, respectively.

strate that the trace to trace variability of measurements on the same chain is quite low. We estimate that we can effectively measure differences in persistence lengths of  $<0.2$  nm and that the trace to trace variability is below this level in a well-controlled experiment.

**Polymer Synthesis and Bulk Characterization.** The preparation of optically switchable polymers for direct observation in molecular force spectroscopy was directed by three basic design parameters: the desire to maximize the potential length change upon irradiation, the need to chemically attach a chain both to the AFM probe tip and to the glass slide substrate, and the need for a sufficiently long chain. The polymer, which we prepared, is a sequential polypeptide with

### Scheme 1. Synthesis of Azobenzene Containing Polypeptides



multiple azobenzene moieties incorporated in the backbone. A heterobifunctionality of the N- and C-termini of the polypeptide chain provides for a gold–cysteine bond to the probe tip and an amide bond to an amino-functionalized surface.

For the incorporation of multiple azobenzene moieties into a linear polymer a sequential polypeptide approach based on polycondensation of tripeptide monomers containing (4-aminomethyl)phenylazobenzoic acid (AMPB)<sup>57,58</sup> was selected. For this purpose, the pentafluorophenyl ester of the pseudo-tripeptide **1** was synthesized in stepwise manner by classical procedures in solution (Scheme 1) and isolated as hydrogen chloride salt (homogeneous on HPLC:  $t_R = 10.4$  min [Nucleosil 100-5 C18 (Macherey & Nagel, Germany); linear gradient of 2%  $\text{H}_3\text{PO}_4$ /acetonitrile from 95:5 to 10:90 in 13 min]; ESI-MS:  $m/z$  785.4 [M + H];  $M_r$  784.3 calculated for  $\text{C}_{39}\text{H}_{41}\text{N}_6\text{O}_6\text{F}_5$ ). Polycondensation of **1** was allowed to proceed in DMF at 0.4 M concentration and at room temperature for 24 h upon addition of 1.2 equiv of triethylamine. The resulting crude polymer was reacted with an excess of Fmoc-Cys(Trt)-OSu in DMF, and after 24 h, the reaction mixture was chromatographed on a phenogel 1K-75K (Phenomenex, Germany) column (300  $\times$  7.8 mm) with DMF at 60  $^\circ\text{C}$  as eluent. The main fraction of  $\sim 25$  kDa molecular weight was collected and reacted with diethylamine for cleavage of the *N*-Fmoc group and generation of polymer **2**. Quantitative comparison of NH and  $\text{C}^\alpha\text{H}$  proton signals in  $^1\text{H}$  NMR spectra of the carboxy-terminal glycine residue with those of all other glycines allowed to estimate an average polycondensation degree of 28. NMR spectra also confirmed hydrolysis of the carboxy-terminal pentafluorophenyl ester during workup and isolation steps of the polymer.

From studies performed on azobenzene<sup>59</sup> as well as on peptides containing the AMPB moiety,<sup>60,61</sup> it is known that *cis*/*trans* photoisomerization of the azobenzene unit is reversible upon irradiation at  $\lambda = 365$  and 450 nm, respectively. However, although the *trans*-azo isomer is obtained upon thermal relaxation in the dark, because of the spectral overlap of the excitations of *cis*- and *trans*-azo isomers, complete photoisomerization upon optical pumping is not possible. The maximum populations that are typically obtained in azobenzene-containing peptides are 70–80% of the *trans*- or *cis*-azo isomer;<sup>58</sup> for convenience, here, we refer to the saturated extended and the saturated short polymer configurations, as the dominant *trans*-azo state and *cis*-azo state, respectively. Upon thermal relaxation into the *all-trans*-azo configuration, the average contour length of the polymer was estimated at 54 nm.

**Sample Preparation and Optomechanical AFM Experiments on Polyazopeptides.** A stepwise attachment of the azobenzene containing polypeptide was utilized to prepare the sample for force measurements. The polymer was first attached to a gold-coated probe tip via the thiol group of the amino-terminal cysteine residue, and then the carboxy-terminal end was covalently bound to amino functionalities on the sample slide. Polymer chains were coupled to the probe tip by first physisorbing them to the cantilevers in DMSO solution, followed by deprotection of the cysteine thiol group



using 5% trifluoroacetic acid in  $\text{CH}_2\text{Cl}_2$ . The proximity of the deprotected thiol groups to the gold surface resulted in chemisorption of the polypeptides to the gold-coated tip via the formation of a covalent Au–S bond.

Flint glass microscope slides were functionalized with *N*-[3-(trimethoxysilyl)propyl]diethylenetriamine (Aldrich) to introduce amino groups. A drop of silane was placed on the slides, which were then placed in a 90 °C oven for 15 min. The slides were rinsed with ethanol followed by water and then placed in 90 °C water for 30 min.

After mounting a polymer modified cantilever chip in the force spectrometer, the carboxy termini of the polypeptides were activated by the addition of 10  $\mu\text{L}$  of a 100 mM *N*-hydroxysuccinimide (NHS) and 1-ethyl-3-(3-(dimethylamino)propyl)carbodiimide (EDC) (NHS and EDC in 1:1 molar ratio) solution in DMSO to promote the formation of an amide bond with the amino groups on the glass slide surface. The cantilever tip with the activated, chemisorbed polymers was brought into contact with the amino-functionalized slide. The formation of a covalent bond was reflected by rupture forces in the nanonewton range,<sup>46</sup> which allowed us to stretch and hold the polymers with a force of several hundred piconewtons for several minutes without bond rupture. Adhesion of short strands of nonspecifically bound polymer was ruptured until a single covalently bound strand remained, at which point we could irradiate and make multiple measurements on a single polymer molecule.

We observed that the stability of the tip and surface attachment of single polypeptide chains is drastically reduced if the polymer is kept at elevated forces for prolonged times. The reported value of 1.4 nN for the failure of gold–sulfur bonds<sup>46</sup> provides an upper limit of the forces we can expect to obtain with the current bifunctional attachment system. If one considers the occurrence of occasional mechanical noise and the addition of mechanical energy to the system from the light pulse, it is not surprising that, on time scales of the experiments, we are limited to forces on the order of 1 nN. Indeed, as the force applied in the experiment rose above 500 pN, the stability of polymer attachment was observed to decrease substantially. Nonetheless, with care we were able to keep an individual chain attached for more than an hour of continuous measurements.

**Data Collection and Analysis.** The data were collected as cantilever deflection and measured piezo position at rates as high as 5 kHz. These data were converted to force and tip–sample separation using the measured spring constant, sensitivity, and point of tip–sample contact. We collected data in Igor Pro (Wavemetrics) as individual force curves or, alternatively, collected 5–10 min of continuously streamed data. The advantage of continuously collecting data was the ability to accurately account for instrument drift during and between many force curves without having to come into contact with the surface between each trace. Corrections in the data were made for low-frequency noise, i.e., thermal effects and instrument creep.

To determine the contour lengths of stretched polypeptide chains, the experimental curves were fitted by an extended wormlike chain (WLC) model including linear elastic contributions arising from the stretching of bond angles and covalent bonds.<sup>62</sup>

$$F \frac{L_p}{k_B T} = \frac{R_z}{L} - \frac{F}{K_0} + \frac{1}{4(1 - R_z/L + F/K_0)^2} - \frac{1}{4} \quad (1)$$

In this expression,  $R_z$  is the measured end–end distance at any given force,  $F$ , and  $L$  is the contour length of the stretched chain (polymer strand) under zero force ( $F=0$ ). The polymer's bending rigidity is expressed by the chain's persistence length,  $L_p$ , and the chain's extensibility upon stretching is described by the segment elasticity,  $K_0$ , which is introduced into eq 1 as a linear term. ( $K_0$  can be understood as the inverse of the normalized compliance of a Hookean spring; the spring constant of the polymer chain is given by  $K_0/L$ .) Note that eq 1 is only based on an approximation to the exact solution of

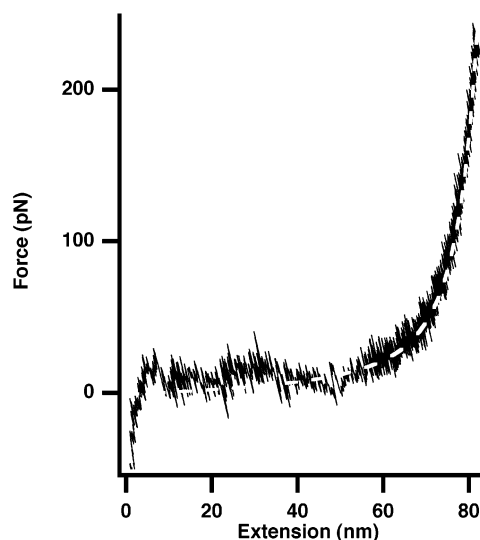


**Figure 4.** Force vs extension trace of a *trans*-azo polypeptide. A wormlike chain (WLC) fit shown by the dashed line reveals a contour length of 89.1 nm, a persistence length of 0.5 nm, and a segment elasticity of 20 000 pN.

the WLC model, which is valid in the range of low and high forces (in the regimes  $F < 1$  pN and  $F > 20$  pN), but may differ in the intermediate regime by as much as 10%.<sup>63</sup> It has been suggested that the extensibility of the polymer chain may be determined from the slope of the linear regime found at forces above several hundred piconewtons,<sup>64</sup> but as this regime is not always accessed, the established WLC fits were used to make comparisons in this investigation.

## Results

**Mechanical Characterization of *all-trans*-Azo-benzene Polymers.** The characteristic shape of a single azobenzene containing polypeptide was established by obtaining numerous force spectra of several individual chains. Figure 4 shows a typical force vs extension plot of a polyazopeptide in the *trans*-azo state; that is its fully extended configuration. The polymer exhibits no measurable conformational transitions, indicating that no significant thermal activation barriers are overcome along the trajectory of mechanical stretching.

The measure for the contour length of a stretched chain is obtained from the extended wormlike chain fit (WLC), after the two other free parameters, persistence length  $L_p$  and segment elasticity,  $K_0$ , were determined. For the force profile of the polyazopeptide in its extended state, we obtained reasonable WLC fits with  $L_p = 0.5$  nm and  $K_0 = 20\,000$  pN. (For the particular polymer molecule shown in this trace, the contour length of  $L = 89.1$  nm was fit; note that the deviation from the average length is due to the molecular weight distribution of the material.) We assumed that the *trans/cis* isomerization does not significantly affect these two parameters, so they were held fixed in all fits to the experimental force–extension curves in order to obtain precise relative values for the contour lengths of polyazopeptides in different configurational states.

**Reversible Optical Switching at Low Force.** Figure 5A shows typical data obtained in a force experiment during which optical excitation was coupled into the sample. The traces are extracted from data streams of cantilever deflection vs time that are recorded. In the time traces, individual light pulses can be observed as spikes in the deflection data. The reader

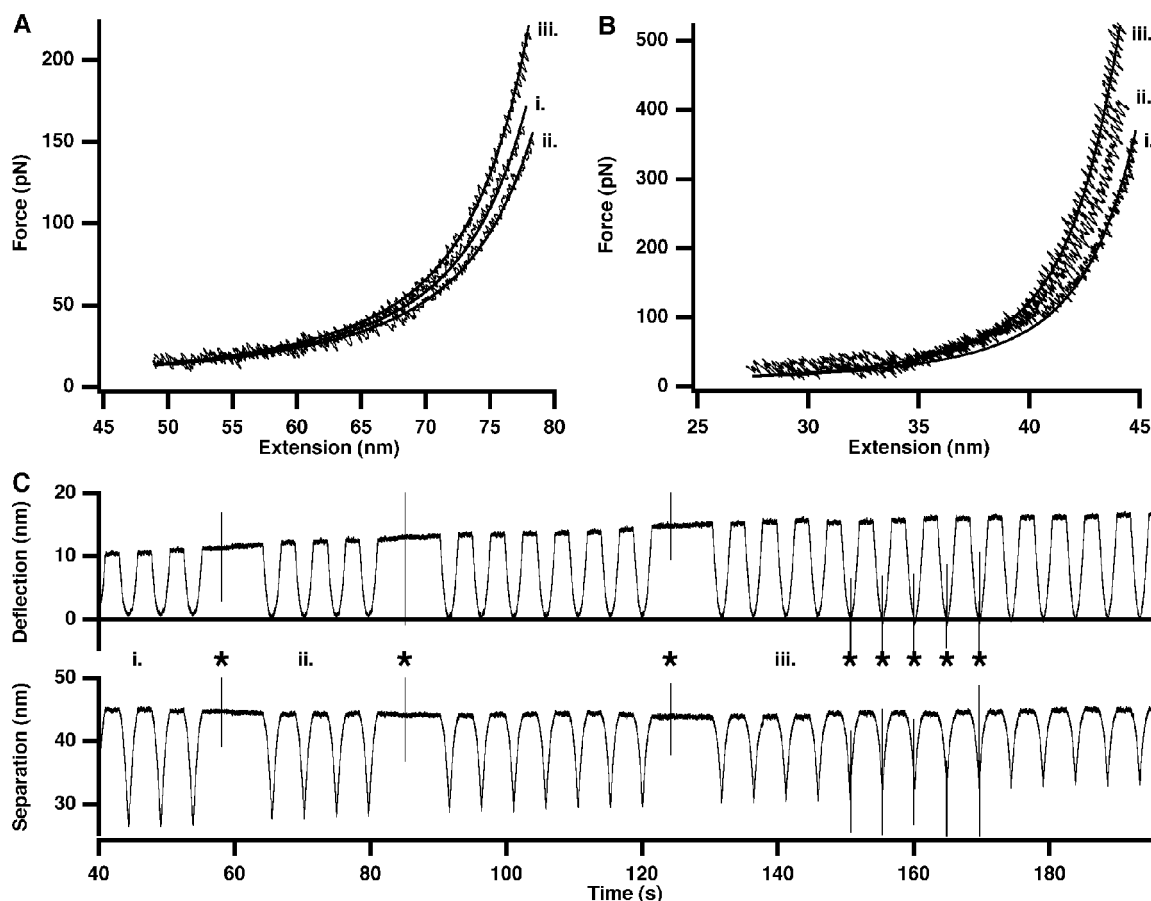


**Figure 5.** Switching azobenzene configurations. (A) Reversible switching of contour length at low forces is demonstrated by the conversion of these data to force vs extension revealing the original trace (i), the more extended trace (ii) after pulses of 420 nm wavelength light drove the polymer to the *trans*-azo configuration, and a shortened trace (iii) after pulses of 365 nm wavelength light drove the polymer to its *cis*-azo configuration. (B) A similar extent of shortening of the polymer chain is observed for a polymer held under external force during excitation. The polymer initially driven to the *trans*-azo state by 420 nm wavelength light (i) is shortened (ii) upon a single flash of 365 nm wavelength light. Two more flashes result in slightly more shortening. Five further flashes at low force do not alter the length. (C) The cantilever deflection vs time for the data displayed in (B) shows the time course of the experiment. Force curves are observed as the gradual increase and decrease in deflection, while the sharp spikes (noted with stars) indicate the light pulses.

is reminded that these spikes result from stray light reflected onto the photodiode and *not* from actual cantilever movement (see experimental part for detailed discussion of artifacts). This signal provides a convenient marker for when the light pulses occurred.

The effect of the light pulses on a single azobenzene polymer can be observed by comparing the force–extension traces extracted prior to and after irradiation of the sample. At the beginning of the experiment, the polymer sample assumed an undefined configurationally mixed state owing to the absorbed ambient radiation. Trace i in Figure 5A is the polymer in this initial mixed state. After five pulses of 430 nm wavelength light, the polymer chain was driven into the saturated extended *trans*-azo state. Trace ii illustrates the lengthening of the polymer due to this switch. The polymer was then driven into the saturated *cis*-azo state by irradiation of five pulses of 365 nm wavelength light. As a result, the polymer exhibited marked shortening as observed in trace iii. Such lengthening and shortening could be repeated several times before the polymer or its attachment to tip or substrate ruptured. The intensity of the light pulses from the flash lamp on the molecule varies to some degree, and so the direct correlation of molecular length change to the number or relative intensity of the light flashes has not yet been possible. However,

we could use several flashes to drive the system into an equilibrium state. We observed that three flashes were enough to reach such a photochemical equilibrium.

Repeated measurements of a particular configurational state of the same polyazopeptide molecule (i.e., no optical excitation between successive measurements) resulted in identical force–extension, even when the time span between successive measurements was minutes. The drift stability of the experimental setup is therefore sufficient to ensure the accurate determination of contour lengths of different polymer configurations based on the WLC fit as described above. A contour length,  $L_{cis} = 83.7$ , was obtained by fitting the *cis*-azo state trace in Figure 5A with a persistence length  $L_p = 0.5$  nm and a polymer segment elasticity of  $K_0 = 20\,000$  pN as described above. From this, the difference in contour lengths ( $\Delta L$ ) between the saturated *trans*- and *cis*-azo states was measured to be 2.8 nm, which corresponds to a relative length change ( $\Delta L/L_{trans}$ ) of  $\sim 3\%$ . Interestingly, stretching of the polymer in its saturated short conformation, despite being the thermodynamically unfavored state, does not result in any mechanically induced configurational transition. The lifetime of the *cis* state is thus still high enough to provide mechanical stability of the short polymer configuration on the time scale of the AFM experiment even

at elevated forces up to 1 nN. The *cis*/*trans* isomerization of polyazopeptides does not result in different shape characteristics of the force curves and is therefore only identified by the relative length changes prior to and after optical irradiation.

**Reversible Optical Switching against External Mechanical Force.** Further experiments were carried out to test whether the configuration of the azo units could be optically switched, while holding the polymer under relatively high tension. Under this condition, optical switching is of particular interest, as the contraction of a polymer chain against an external force may be employed for an optomechanical energy conversion at the single-molecule level. Figure 5B,C shows the results of one such experiment. The streamed deflection and molecular extension data are displayed in Figure 5C. The sharp spikes show the points when light was flashed into the system. The labeled force curves showing decreases in extension correspond to the extracted force curves displayed in Figure 5B. Prior to the experiment, we drove the polymer into the saturated *trans*-azo conformation with five consecutive flashes at 420 nm. Trace i reveals that, in the saturated *trans*-azo state, this polymer molecule's contour length is 47.7 nm. The molecule was stretched to a force of about 350 pN, and a single 365 nm pulse at constant tip-sample separation resulted in a shortening by about 1.0 nm, as measured from trace ii. Two further pulses holding the polymer at the slightly higher force resulted in an additional shortening by 0.9 nm observed in trace iii. Since five additional 365 nm wavelength pulses at low force did not result in further shortening, the polymer was assumed to be in the saturated *cis*-azo state. The relative length change observed here against external force between the two saturated states corresponds well with the value found for *trans*- to *cis*-azo switching at low force ( $\Delta L/L_{\text{trans}} \sim 3\%$ ). Only at very high forces do we find hints for a suppression of the optical *trans*/*cis* isomerization reaction. However, because of the limited stability of polymer-surface attachment at high forces, we have relatively few data at these high forces. The highest force at which contraction of polymer was clearly observed was 400 pN.

## Discussion

**Mechanical Stability of Azobenzene Configurations.** The rate at which an equilibrium is reached (i.e., the lifetime,  $\tau$ , of any initially populated configurational state) depends on the activation barrier of the transition between the different states,  $\Delta G^*$ . For AMPB peptides in DMSO an activation energy barrier for thermal reisomerization from the *cis*- to the *trans*-isomer of  $\Delta G^* = 44 \pm 2 k_B T$  has been determined.<sup>60</sup> The experimentally determined lifetime of the *cis*-azo configuration at 301 K is 120 h.<sup>60</sup>

At the time scale of a single AFM stretching experiment, any state with  $\tau_0$  greater than 1 min can be considered "stable". However, the mechanical energy applied by stretching alters the conformational potential landscape by effectively tilting it along the stretching coordinate. This reduces the activation barrier of any transition that proceeds in the direction of a path nonorthogonal to the applied force. Therefore, the probability, and thus also the rate, of such a transition increases as the lifetime of the initial state decreases. It can be estimated from the Bell equation<sup>65</sup>

$$\tau_F = \tau_0 \exp[(-F_z \Delta z^*)/k_B T] \quad (2)$$

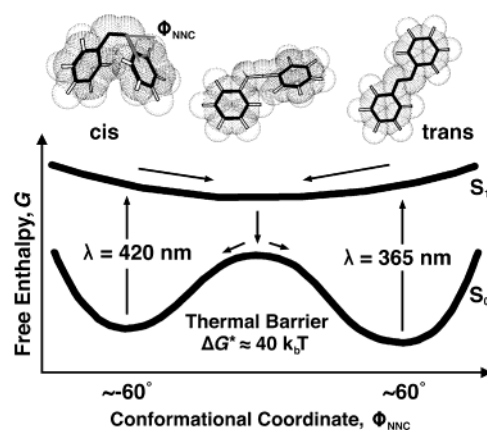


**Figure 6.** Schematics of a cut through the potential energy landscape of the reversible azobenzene *cis*/*trans* transition along the inversion pathway. The relevant conformational coordinate is the bond angle which changes from about  $-60^\circ$  to  $+60^\circ$  for an in-plane transition of the right phenyl ring from the *cis*- to the *trans*-azo position.<sup>60,66,67</sup> The transition can be induced by optical excitation (*cis*-azo form at 420 nm; *trans*-azo form at 365 nm). Typically, the *trans*-azo form is thermally favored. (The graph is based on previous theoretical<sup>66</sup> and experimental data.<sup>68,69</sup>)

in which  $F_z$  is the projection of the applied force along the internal transition coordinate  $z$  and  $\Delta z^*$  is the "width" of the conformational transition potential. The length difference in the end-to-end distance of a single azobenzene unit in the *cis*- and *trans*-azo states was calculated ab initio using the INSIGHT II software ( $l_{\text{trans}} \sim 1.9$  nm,  $l_{\text{cis}} \sim 1.65$  nm, and therefore  $\Delta l \sim 0.25$  nm). Then assuming a symmetric potential,  $\Delta z^*$  is  $\sim 0.13$  nm. According to the Bell equation, the lifetime of the excited *cis*-isomer is reduced to  $\tau_F \sim 100$  ms, once the projection of the stretching force on the coordinate describing the trajectory of the *cis*/*trans* transition exceeds 400 pN. While this force is well within the range of stretching forces applied in our AFM experiments, the saturated *cis*- and *trans*-azo configurations were both found mechanically stable to all experimental pulling forces on the time scale of the experiment. For the lower energy *trans*-azo configuration, this is expected, as it represents the equilibrium configurational state.

A likely explanation for the somewhat surprisingly high stability of the *cis*-azo configuration is that the force-induced transition proceeds along a pathway nearly orthogonal to the thermal *cis*/*trans* isomerization. The activation barrier and thus the thermal lifetime of the *cis*-azo configuration would remain unaltered. Note that the thermal *cis*/*trans* isomerization is suggested to proceed along an isomerization pathway in which the dihedral angle  $\Phi_{\text{NNC}}$  is the relevant configuration coordinate (Figure 6)<sup>60,66–69</sup> and that, the azo groups are not all aligned with the stretching coordinate. A more generalized view of this effect would be that the forced transition occurs on a pathway ensemble whose width in conformation space is drastically restricted by the external force acting along the polymer backbone. The thermal transition, however, samples the whole conformation space and may reach saddles and low-energy barriers, which are not accessible for the forced transition. This would to a certain degree correspond to the conformationally locked interaction found in certain biopolymers, e.g., actin filaments, which are known to withstand forces of up to 100 pN for seconds although their equilibrium constant is in the millimolar range.



If there is such a separate mechanical pathway, our measurements allow us to set a lower bound for the lifetime,  $\tau_{0,z}$  of the *cis*-azo state when restricted to this path along the stretching coordinate  $z$ . With eq 2 and the observation that a molecule can be held in the *cis*-azo state at forces of  $\sim 1$  nN for longer than a second, it is estimated as  $\tau_{0,z} \sim 3 \times 10^{13}$  s (i.e.,  $\sim 1$  million years). The lifetime of a state,  $\tau_0$ , is correlated with the energy barrier of the escape path,  $\Delta G^*$ , via  $\tau_0 = (1/\nu_0) \exp(-\Delta G^*/k_B T)$ ,<sup>70</sup> where  $\nu_0$  may be seen as a characteristic frequency of the transition.<sup>71</sup> If  $\nu_0$  is assumed independent of the pathway, the energy barrier  $\Delta G_\Phi^*$  along the configurational coordinate  $\Phi_{\text{NNC}}$  and the energy barrier  $\Delta G_z^*$  along the stretching coordinate  $z$  are related by

$$\Delta G_z^* = \Delta G_\Phi^* + k_B T \ln(\tau_{0,z}/\tau_{0,\Phi}) \quad (3)$$

Thus,  $\Delta G_z^* \sim 62 k_B T$ ; i.e., the energy barrier is increased by approximately  $18 k_B T$  when the molecules' escape path is restricted to the stretching coordinate. However, these estimates are based on the assumption that the natural frequency  $\nu_0$  is the same in the forced and the thermal process. This need not necessarily be the case. Particularly on top of the saddle where the state density is drastically reduced, the transition state theory may break down. Our finding of the unexpected stability of the *cis*-azo state against external force may reflect this effect.

**Photochemically Induced Length Changes and Mechanical Work.** The lengths of a single azotripeptide unit in the *cis*- and the *trans*-azo state from theoretical calculations are  $l_{\text{trans}} \sim 1.9$  nm and  $l_{\text{cis}} \sim 1.65$  nm. As discussed above, the spectral overlap of the excitations of *cis*- and *trans*-azo configurations limits the photochemical switching of polyazopeptides to shifting the average configurational populations between the two limits  $\sim 80\%$  *trans*-azo and  $\sim 75\%$  *cis*-azo state.<sup>60</sup> From this, we may give an "average monomer length" in the polymer's saturated *trans*-azo state as  $\langle l_{\text{trans}} \rangle \sim 1.85$  nm. In the saturated *cis*-azo state, a total average of 55% azobenzene units change their configuration, which corresponds to an average contraction,  $\langle \Delta l \rangle \sim 0.14$  nm, or an average monomer length in the polymer's saturated *cis*-azo state,  $\langle l_{\text{cis}} \rangle \sim 1.71$  nm.

The fitted contour length of the polyazopeptide molecule in Figure 5A is  $L_{\text{trans}} \sim 86.5$  nm in its saturated *trans*-azo state, as obtained from the WLC fit to our data. This corresponds to 46 azotripeptide monomers. Considering the theoretical contraction per monomer of 0.14 nm, a maximum contraction,  $\Delta L_{\text{max}}$ , of 6.4 nm, a relative change of 7.4%, could be expected by optical pumping at 365 nm. The actual length change measured at saturation at low forces is 2.8 nm ( $\sim 3\%$ ), which is considerably less than this upper limit. The difference may reflect the fact that some parts of the polymer chain are not excited by the evanescent field. More importantly, the above calculations on the monomer lengths do not directly correlate to the contour length of the polymer chain. Intrinsic viscosity measurements on azobenzene polymers have shown the largest effects of optical excitation on the end–end distance of the polymer coils in solution, when the photoactive units were connected by stiff rather than flexible chain segments.<sup>22,23</sup> In our experiments, the polymer chains are fixed between tip and substrate and stretched beyond the coil regime. While this geometry is thus more comparable with photoactive bulk polymer networks, which may show considerable length changes

upon optical switching,<sup>27</sup> the remaining conformational freedom of the polypeptide backbone may compensate for some of the azobenzene shortening by rotations around single backbone bonds.<sup>60</sup>

In other words, orientational rearrangement of the azobenzene units, such as a change in their tilt angle with respect to the polymer main axis, remain possible in order to compensate for some of the conformational strain induced by the configurational change. Additionally, the *cis*-azo configuration could have a lower chain elasticity than the *trans*-azo configuration, which would result in lower measured length change upon extension than expected. As a result, the maximum contraction of the azobenzene unit  $\Delta l$  is thus not entirely projected onto the stretching axis. The experimentally measured absolute length change of the polyazopeptide relates to an averaged contraction of  $\langle \Delta l \rangle = 0.06$  nm per monomer in contour length. As only 55% of the azobenzene units change their configuration, the length change of a single azobenzene unit upon *trans*- to *cis*-azo switching, which is detectable along the stretching axis, is estimated as  $\Delta F = 0.11$  nm.

**Efficiency of Converting Optical Excitation Energy to Mechanical Work.** It is instructive to have a look at the efficiency of the optomechanical energy conversion in the limit of all light reaching the polymer in order to describe the experimental limit of efficiency. In Figure 5A, contraction against a force of about 400 pN is shown, resulting in an average shortening of 0.12 nm per azobenzene monomer. When one assumes that each switching of a single azobenzene unit is initiated by a single photon carrying an energy of  $h\nu = 5.5 \times 10^{-19}$  J ( $\lambda = 365$  nm), the conversion of this photon to mechanical work has an efficiency of about 10%.<sup>72</sup> This estimate neglects that the azobenzene is not excited by every photon that it interacts with. (The quantum yield is about 10% for *trans*- to *cis*-azo.) In addition, to lengthen the shortened polymer and complete a cycle, a second photon ( $h\nu = 4.7 \times 10^{-19}$  J,  $\lambda = 430$  nm) is absorbed at a quantum yield of about 50%. With about 10 azobenzene units in the chain measured in the cycle,<sup>72</sup> about 120 photons or an energy of  $6.6 \times 10^{-17}$  J is needed for one complete cycle. The total mechanical energy transduced to the cantilever is about  $5 \times 10^{-20}$  J (estimated from the area of the cycle). This results in a total efficiency of about  $7.5 \times 10^{-4}$  for this extremely simple optomechanical motor. This is only a rough estimate of efficiency, and we recognize that there are many other effects that will complicate more accurate estimates of efficiency, including thermal back-relaxation, the field strength, and orientation dependency of excitation efficiency, etc.

## Conclusions

We have demonstrated the incorporation of a chromophore into a polymer chain allowing controlled lengthening and shortening of the chain contour length and the ability to read out this change in a single polymer with a macroscopic device. Not only was this accomplished in a relaxed chain, but also while the chain was held extended by an external force. In the extended state, the shortening transition was able to convert the absorbed optical energy into mechanical work performed on the system. We demonstrated that such a molecule could be used for a molecular switch via length change or to perform work on a system.

The use of optomechanical energy conversion for molecular switches is promising since the light can be

applied in a controlled, clean manner. One must only be concerned with thermal effects. The coupling of optical excitation into polymer mechanics therefore seems to be the most attractive approach for the general study of energy transductions at the single molecule level. We have recently demonstrated that the mechanical stability of the two different azobenzene configurations is sufficient to operate the experiment in an optomechanical cycle and thus to perform work at the molecular level.<sup>72</sup>

Our results prepare the way for the development of improved optomechanical switches with higher activation barriers, such as could be provided by structural units, in which covalent bonds are formed and cleaved during the reversible photochemical process. Most prominent examples are spiropyranes and spirooxazines, fulgides and fulgimides, and some diarylethene derivatives, but their introduction into polymer main chains (which would be needed for their study by AFM force spectroscopy) appears synthetically much more demanding.

Not to be overshadowed by the thoughts of building nanomachines, this experimental system is a promising method for quantifying how an applied force can alter the energy landscape of chromophore transitions. This could provide new fundamental insights into the course of photoreactions under external loads. Investigating the dependence of the transitions on the excitation wavelength and external load will require carefully planned experiments since the complexity of the potential mechanisms is confounded by contributions of alignment of the chromophores, the exponentially decaying field strength (in addition to the possibility of near field amplification of the light by the AFM probe), and the small contour length changes. But a systematic wavelength-dependent analysis would allow the mapping of the energy landscape as a function of external force and chromophore substitution pattern.

**Acknowledgment.** We thank R. Netz, H. Grubmüller, J. Kreuzer, and W. Zinth for helpful discussions as well as Asylum Research for technical support. The study was supported by the Deutsche Forschungsgemeinschaft (DFG), the Humboldt Foundation, and the Fonds der Chemischen Industrie.

## References and Notes

- Brown, C. H. *Photochromism*; Wiley-Interscience: New York, 1971.
- Rau, H. In *Photochromism: Molecules and Systems*; Dürr, H., Bouas-Laurent, H., Eds.; Elsevier: Amsterdam, 1990; Vol. 40, pp 165–192.
- Irie, M. *Photoreactive Materials for Ultrahigh-Density Optical Memory*; Elsevier: Amsterdam, 1994.
- Feringa, B. L.; Jager, W. F.; de Lange, B. *Tetrahedron* **1993**, *49*, 8267–8310.
- Tamai, N.; Miyasaka, H. *Chem. Rev.* **2000**, *100*, 1875–1890.
- Hartley, G. S. *Nature (London)* **1937**, *140*, 281.
- Shinkai, S.; Manabe, O. *Top. Curr. Chem.* **1984**, *121*, 67–104.
- Willner, I. *Acc. Chem. Res.* **1997**, *30*, 347–356.
- Ulysse, L.; Cubillos, J.; Chmielewski, J. *J. Am. Chem. Soc.* **1995**, *117*, 8466–8467.
- Asanuma, H.; Ito, T.; Yoshida, T.; Liang, X.; Komiyama, M. *Angew. Chem., Int. Ed.* **1999**, *38*, 2393–2395.
- Kumar, G. S.; Neckers, D. C. *Chem. Rev.* **1989**, *89*, 1915–1925.
- Irie, M. *Adv. Polym. Sci.* **1990**, *94*, 27–67.
- Vögtle, F. *Supramolecular Chemistry*; Wiley: New York, 1991.
- Würthner, F.; Rebek Jr., J. *J. Chem. Soc., Perkin Trans. 2* **1995**, 1727–1734.
- Archut, A.; Azzellini, G. C.; Balzani, V.; De Cola, L.; Vögtle, F. *J. Am. Chem. Soc.* **1998**, *120*, 12187–12191.
- Ikeda, T.; Tsutsumi, O. *Science* **1995**, *268*, 1873–1875.
- Eich, M.; Wendorff, J. H.; Reck, B.; Ringsdorf, H. *Makromol. Chem. Rapid Commun.* **1987**, *8*, 59–63.
- Eich, M.; Wendorff, J. H. *Makromol. Chem. Rapid Commun.* **1987**, *8*, 467–471.
- Bieringer, T.; Wuttke, R.; Gessner, U.; Rübner, J.; Haarer, D. *Macromol. Chem. Phys.* **1995**, *196*, 1375–1390.
- Zilker, S. J.; Bieringer, T.; Haarer, D.; Stein, R. S.; van Egmond, J. W.; Kostromine, S. G. *Adv. Mater.* **1998**, *10*, 855–859.
- Eisenbach, C. D. *Polymer* **1980**, *21*, 1175–1179.
- Blair, H. S.; Pogue, H. I.; Riordan, E. *Polymer* **1980**, *21*, 1195–1198.
- Irie, M.; Hirano, Y.; Hashimoto, S.; Hayashi, K. *Macromolecules* **1981**, *14*, 262–267.
- Strzegowski, L. A.; Martinez, M. B.; Gowda, D. C.; Urry, D. W.; Tirrell, D. A. *J. Am. Chem. Soc.* **1994**, *116*, 813–814.
- Laguné Labarthe, F.; Bruneel, J. L.; Buffeteau, T.; Sourisseau, C.; Huber, M. R.; Zilker, S. J.; Bieringer, T. *Phys. Chem. Chem. Phys.* **2000**, *2*, 5154–5167.
- Schulz, B. M.; Huber, M. R.; Bieringer, T.; Krausch, G.; Zilker, S. J. *Synth. Met.* **2001**, *124*, 155–157.
- Finkelmann, H.; Nishikawa, E.; Pereira, G. G.; Warner, M. *Phys. Rev. Lett.* **2001**, *87*, 015501–015504.
- Oster, G.; Wang, H. In *ATP Synthase: The rotary molecular motors working together*; Creighton, T., Ed.; Wiley: New York, 1999.
- Vale, R. D.; Milligan, R. A. *Science* **2000**, *288*, 88–95.
- Keller, D.; Bustamante, C. *Biophys. J.* **2000**, *78*, 541–556.
- Bustamante, C.; Keller, D.; Oster, G. *Acc. Chem. Res.* **2001**, *34*, 412–420.
- Howard, J. *Mechanics of Motor Proteins and the Cytoskeleton*; Sinauer Assoc.: Sunderland, MA, 2001.
- Balzani, V.; Credi, A.; Raymo, F. M.; Stoddart, J. F. *Angew. Chem., Int. Ed.* **2000**, *39*, 3348–3391.
- Feringa, B. L.; van Delden, R. A.; Koumura, N.; Geertsema, E. M. *Chem. Rev.* **2000**, *100*, 1789–1816.
- Collin, J. P.; Dietrich-Buchecker, C.; Gaviña, P.; Jimenez-Molero, M. C.; Sauvage, J. P. *Acc. Chem. Res.* **2001**, *34*, 477–487.
- Pease, A. R.; Jeppesen, J. O.; Stoddart, J. F.; Luo, Y.; Collier, C. P.; Heath, J. R. *Acc. Chem. Res.* **2001**, *34*, 433–444.
- Schalley, C. A.; Beizai, K.; Vögtle, F. *Acc. Chem. Res.* **2001**, *34*, 465–476.
- Shipway, A. N.; Willner, I. *Acc. Chem. Res.* **2001**, *34*, 421–432.
- Balzani, V.; Credi, A.; Venturi, M. *Proc. Natl. Acad. Sci. U.S.A.* **2002**, *99*, 4814–4817.
- Ballardini, R.; Balzani, V.; Credi, A.; Gandolfi, M. T.; Venturi, M. *Acc. Chem. Res.* **2001**, *34*, 445–455.
- Kishino, A.; Yanagida, T. *Nature (London)* **1988**, *334*, 74–76.
- Ashkin, A.; Schütze, K.; Dziedzic, J. M.; Euteneuer, U.; Schliwa, M. *Nature (London)* **1990**, *348*, 346–348.
- Smith, S. B.; Finzi, L.; Bustamante, C. *Science* **1992**, *258*, 1122–1126.
- Sheetz, M. P. *Laser Tweezers in Cell Biology*; Academic Press: New York, 1997.
- Binnig, G.; Quate, C. F.; Gerber, C. *Phys. Rev. Lett.* **1986**, *56*, 930–933.
- Grandbois, M.; Beyer, M.; Rief, M.; Clausen-Schaumann, H.; Gaub, H. E. *Science* **1999**, *283*, 1727–1730.
- Viani, M. B.; Schaffer, T. E.; Paloczi, G. T.; Pietrasanta, L. I.; Smith, B. L.; Thompson, J. B.; Richter, M.; Rief, M.; Gaub, H. E.; Plaxco, K. W.; Cleland, A. N.; Hansma, H. G.; Hansma, P. K. *Rev. Sci. Instrum.* **1999**, *70*, 4300–4303.
- Clausen-Schaumann, H.; Seitz, M.; Krautbauer, R.; Gaub, H. *Curr. Opin. Chem. Biol.* **2000**, *4*, 524–530.
- Janshoff, A.; Neitzert, M.; Oberdörfer, Y.; Fuchs, H. *Angew. Chem., Int. Ed.* **2000**, *39*, 3212–3237.
- Hugel, T.; Seitz, M. *Macromol. Rapid Commun.* **2001**, *22*, 989–1016.
- Rief, M.; Oesterhelt, F.; Heymann, B.; Gaub, H. E. *Science* **1997**, *275*, 1295–1297.
- Smith, S. B.; Cui, Y.; Bustamante, C. *Science* **1996**, *271*, 795–799.
- Rief, M.; Clausen-Schaumann, H.; Gaub, H. E. *Nat. Struct. Biol.* **1999**, *6*, 346–349.
- Oesterhelt, F.; Rief, M.; Gaub, H. E. *New J. Phys.* **1999**, *1*, 6.1–6.11.



- (55) Rief, M.; Fernandez, J. M.; Gaub, H. E. *Phys. Rev. Lett.* **1998**, *81*, 4764–4767.
- (56) Butt, H. J.; Jaschke, M. *Nanotechnology* **1995**, *6*, 1–7.
- (57) Behrendt, R.; Renner, C.; Schenk, M.; Wang, F.; Wachtveitl, J.; Oesterhelt, D.; Moroder, L. *Angew. Chem., Int. Ed.* **1999**, *38*, 2771–2773.
- (58) Behrendt, R.; Schenk, M.; Musiol, H. J.; Moroder, L. *J. Pept. Sci.* **1999**, *5*, 519–529.
- (59) Rau, H., Rabek, J. F., Eds.; CRC Press: Boca Raton, FL, 1989; Vol. 2, pp 119–141.
- (60) Renner, C.; Cramer, J.; Behrendt, R.; Moroder, L. *Biopolymers* **2000**, *54*, 501–514.
- (61) Renner, C.; Behrendt, R.; Heim, N.; Moroder, L. *Biopolymers* **2002**, *63*, 382–393.
- (62) Bustamante, C.; Marko, J. F.; Siggia, E. D.; Smith, S. *Science* **1994**, *265*, 1599–1600.
- (63) Bouchiat, C.; Wang, M. D.; Allemand, J.-F.; Strick, T.; Block, S. M.; Croquette, V. *Biophys. J.* **1999**, *76*, 409–413.
- (64) Livadaru, L.; Netz, R. R.; Kreuzer, J., submitted to *Macromolecules*.
- (65) Bell, G. I. *Science* **1978**, *200*, 618–627.
- (66) Monti, S.; Orlandi, G.; Palmieri, P. *Chem. Phys.* **1982**, *71*, 87–99.
- (67) Robertson, J. M. *J. Chem. Soc.* **1939**, 232–236.
- (68) Rau, H. *J. Photochem.* **1984**, *26*, 221–225.
- (69) Nägele, T.; Hoche, R.; Zinth, W.; Wachtveitl, J. *Chem. Phys. Lett.* **1997**, *272*, 489–495.
- (70) Arrhenius, S. *Z. Phys. Chem.* **1889**, *4*, 226.
- (71) Hänggi, P.; Talkner, P.; Borkovec, M. *Rev. Mod. Phys.* **1990**, *62*, 251–341.
- (72) Hugel, T.; Holland, N. B.; Cattani, A.; Moroder, L.; Seitz, M.; Gaub, H. E. *Science* **2002**, *296*, 1103–1106.

MA021139S